CrystEngComm

Cite this: *CrystEngComm*, 2011, **13**, 3573

www.rsc.org/crystengcomm

PAPER

Can a computer crystallize a liquid? Molecular simulation of continuous trajectories from liquid to crystalline *n*-hexane†‡

Angelo Gavezzotti*

Received 20th January 2011, Accepted 2nd March 2011
DOI: 10.1039/c1ce05106g

A new algorithm is described for the simulation of the organization processes that lead from an isotropic liquid to a crystal structure. The algorithm is based on a hybrid, pseudo-Monte Carlo technique that lets a molecular assembly evolve under Metropolis conditions subject to forcing the decrease of asymmetry parameters that quantify the deviation from intermolecular alignment. This procedure was applied to the simulation of the liquid–solid transformation in *n*-hexane. Starting from liquid *n*-hexane with a significant population of *gauche* molecular conformations, a crystalline molecular assembly with parallel all-*trans* aliphatic chains is generated. This structure is very similar to the real crystal structure, except for a small difference in molecular orientation within layers. The process apparently involves an activation energy of a few kJ mol^{-1} and a very minor volume activation that could be associated with density fluctuations due to the need for extra space as long molecules undergo a large conformational rearrangement. Although some detailed quantitative aspects of the simulation may be open to discussion, this is one of the very few examples of individuation of a continuous all-atom trajectory linking the liquid and the solid state of a large polyatomic molecule. The results confirm the viability of the symmetry bias for the generation of new crystal structures, and provide valuable working hypotheses on the mechanism of crystallization.

Introduction

The early stages of molecular recognition and aggregation in the liquid or in solution, leading to nucleation of crystals made of organic molecules, are inaccessible to detailed experimental investigation.[1] For molecular weights of the order of 100–500 au the early nuclei are too small, rare and fleeting for the resolution and timescales even of modern instrumentation. Structural or energetic differences between free molecules and aggregate molecules are hardly detectable even by the most sensitive spectroscopies, so that it is extremely difficult to monitor the intimate detail of aggregation processes.

Molecular simulation offers an alternative window on the atomic-scale aspects of molecular pre-organization and of nucleation. This is presently the grand challenge of predictive theoretical chemistry, because for large organic molecules, the time- and size barriers prevent a realistic reproduction of the actual proceedings: simulations cannot be long enough, nor can be applied to large enough systems. Appropriate shortcuts must be devised. This paper introduces a symmetry-biased simulation procedure in which the acceptance of Monte Carlo-Metropolis moves is biased by the request of a decrease in the geometrical asymmetry within the molecular assembly, for which appropriate numerical indices are proposed. By driving the evolution towards the translation–inversion symmetries that are known to exist in all linear *n*-alkane crystals,[2] the procedure is here applied to investigate the atomic detail of the conformational change (chain-straightening) and of the molecular alignment that must occur in the crystallization of liquid *n*-hexane. Semi-crystalline structures with all parallel straight chains are easily generated, and a judicious choice of the simulation protocols and parameters eventually leads to the finding of a continuous path through phase space, connecting isotropic, *trans–gauche* equilibrated liquid with an all-*trans*, long-range ordered aggregate that very closely resembles the *n*-hexane crystal structure. This represents one of the very few direct descriptions of a crystallization trajectory that have ever appeared in the literature.[3,4] Although there may not be certainty that the present choice is the one and only trajectory for the process under investigation, the derived energy, volume and conformational activation parameters are extremely realistic, providing new insights and valuable working hypotheses on the still mysterious process of molecular crystallization.

Department of Structural Chemistry, University of Milano, via Venezian 21, 20133 Milano, Italy. E-mail: angelo.gavezzotti@unimi.it

† The documented source Fortran code and the full atomic coordinates along the described liquid-crystal trajectories can be obtained upon request to the author at his e-mail address.

‡ Electronic supplementary information (ESI) available: Details of the Monte Carlo code and of the torsional force field; Fig. S1–S7, Table S1. See DOI: 10.1039/c1ce05106g

Method

Force fields

Each molecule in the computational box is described by a center-of-mass vector, three rigid-body rotation angles, and a number of internal torsion angles. Bond lengths and bond angles are kept fixed, since the involved vibrational frequencies are irrelevant to the present problem. In the force field the total energy E has a torsional part, $f(\tau)$, a minor intramolecular non-bonded contribution, u(intra), and an intermolecular part, $u(R)$:

$$E = \Sigma f(\tau) + \Sigma u(R) + u(\text{intra}) \quad (1)$$

$$u(R_{ij}) = A \exp(-BR_{ij}) - CR_{ij}^{-6} + 1/(4\pi\varepsilon^{\circ})\, q_i q_j R_{ij}^{-1} \quad (2)$$

$f(\tau)$ for C–C–C–C torsion is a polynomial expansion in τ fitted to experimental *trans–gauche* equilibrium data,[5] or the usual three-fold cosine function for H–C–C–C torsion with a staggered minimum (see details in ESI, Fig. S1‡). The potential (eqn (2)) is formulated in terms of intermolecular atom–atom distances R_{ij}. A, B and C are disposable parameters, specific for each atom-type pair. The intramolecular non-bonded energy is a sum of such terms over atom–atom contacts between ends of the chain, to prevent unrealistic clashes in highly coiled conformations. The q's are atomic charge parameters for a Coulomb-type term, as it turns out quite irrelevant for most of the treatment. Based on extensive previous experience[6,7] we use here an adapted version of the UNI force field,[8] the adaptation consisting in a reduction of the steepness of the repulsion wall and an increase of the depth of the attractive wells. The rescaling is conducted using experimental densities and heats of vaporization as targets. The final parameters for eqn (2) are summarized in Table 1.

Asymmetry indices

For each configuration of the computational box, indices for possible translation or inversion symmetry between pairs of solute molecules are calculated as follows, using an adaptation of a method previously developed to detect pseudosymmetries in crystals.[9] Let N_{atoms} be the number of atoms in each molecule, and N_{mol} the number of molecules in the box. Consider molecule k and each of its $N_{\text{mol}} - 1$ neighbors in the box, denoted by index m. The coordinates of all atoms in the two molecules k and m are referred to a common origin, set at a convenient atomic site (the choice of the site is not influential). When molecules are related by pure translation, all atoms of molecule k overlap the corresponding atoms of molecule m, or (a) $x_{ki} = x_{mi}$, while a perfect inversion center symmetry results in (b) $x_{ki} = -x_{mi}$ for all atoms i in the molecule. Therefore, the two asymmetry indices are:

Table 1 Force field potential parameters: A, B, C for $E = A \exp(-BR) - CR^{-6}$. Distances in Å, energies in kJ mol^{-1}. Charge parameters were assigned as +0.10 electrons for hydrogens, −0.2 and −0.3 electrons for methylene and methyl carbon atoms

	A	B	C
H···H	11393.0	3.750	150.32
H···C	59 447	3.87	524.11
C···C	99 078	3.289	2316.1

$$t_{km} = 1/N_{\text{atoms}} \textstyle\sum_i [(x_{ki} - x_{mi})^2]^{1/2} \text{ translation} \quad (3)$$

$$i_{km} = 1/N_{\text{atoms}} \textstyle\sum_i [(x_{ki} + x_{mi})^2]^{1/2} \text{ inversion} \quad (4)$$

These asymmetry indices are zero for perfect symmetry. They do not depend on the absolute value of the distance between the two molecules, and are homogeneous and comparable, being numbers in Å for an average deviation from symmetry per atom. The k–m molecular pair is assigned the smaller of the two asymmetry indices, called s_{km}. The total asymmetry index for the k-th molecule in the box is the average over all k–m pairs, and the overall index for the whole box is the average over all molecules:

$$S_k = 1/(N_{\text{mol}} - 1)\ \Sigma_m s_{km} \quad (5)$$

$$S_{\text{all}} = 1/N_{\text{mol}} \Sigma_k S_k \quad (6)$$

Each s_{km} index is compared with a given threshold value for translation or inversion symmetry, here 0.5 Å; the molecular pair is tagged as no-symmetry if s_{km} exceeds the thresholds, or as related by translation or by inversion symmetry, if s_{km} is below the corresponding threshold. When symmetry-biased runs are performed, the hierarchy of acceptance is (a) a decrease in the final index (eqn (6)) within the preset tolerance; and (b) the usual Monte Carlo-Metropolis criterion on energies. The symmetrization tolerance index, T_s, provides the main leverage in the conduction of the simulation: too high a tolerance leads to no symmetrization, too small a tolerance leads to unrealistically fast symmetrization without proper simulation "time" for relaxation. The asymmetry decrease is thus the driving force of the simulation, and, in a rather far-fetched interpretation of uncertain rigorousness, it could be interpreted as an alias for the decrease in entropy during crystallization.

Simulation procedures

Simulations are performed with periodic boundary conditions: whenever the center of mass of a molecule exits the computational box, the whole molecule re-enters from the opposite side of the box. Intermolecular energies are given by summations of terms as in eqn (2) over atom–atom pairs in different molecules, including all molecules in the box, plus molecules repeated by box periodicity, up to a threshold of 20 Å in the distance between centers of mass.

Molecular dynamics is not well suited for the present purpose, because biasing its deterministic equations is very difficult both conceptually and from the computational point of view. Monte Carlo is more easily biased, but the standard NPT pressure control[10] with fixed pressure is not suited to allow for possible expansions and contractions in the course of the simulation. As a compromise, Monte Carlo was chosen, but the isotropic pressure control is applied by a coupling procedure similar to one used in molecular dynamics,[11] *via* an evaluation of the molecular virial; interatomic forces are evaluated from the derivatives of the potentials (see ESI‡ for more details). The pressure control procedure is applied at pre-selected intervals, typically 1000 MC moves. The crystal structure of *n*-hexane[2] was simulated with box periodicity but at constant volume and temperature, only to estimate the sublimation energy and the order of magnitude of the asymmetry index generated by molecular libration. The

gaseous state was simulated by a MC run on a single molecule *in vacuo*.

Runs for the liquid state of *n*-hexane were performed starting from a computational box of 1024 molecules prepared with a random distribution of centers of mass, orientation angles and torsion angles. Extensive optimization and equilibration runs with pressure control were carried out prior to the final production runs. The lowest temperature was chosen as slightly below the solidification temperature (178 K) in order to have a supercooled liquid for the subsequent simulations of crystallization. The equilibrated box at 160 K was taken as the starting point for the simulation of the pure liquid at 200, 240 and 290 K in successive warm-up runs. The crystal was simulated at a constant volume at 100 and 160 K using the experimental cell dimensions,[2] in a box with 792 molecules (12 × 11 × 6 cell repetitions).

Vaporization and sublimation energies are estimated as differences between total configurational energies of the condensed and gaseous states, as $\Delta H = (U_{gas} - U_{cond}) + RT$. Given the small population of *gauche* conformers, intramolecular energy differences are small but non-negligible. Radial distribution functions are calculated in the usual way,[12] and scattering profiles of given simulation frames are calculated by the Debye equation.[13] The results described in the present paper have been obtained by a computer code written *de novo* for the specific purpose, as described also in a parallel contribution[14] (dealing with a completely different topic). An unspecific personal PC running in an MS-DOS environment has been employed. A typical simulation on a 10 000 atom computational box with full volume and pressure control runs 1 Mmove = 10^6 MC moves in about 1 hour for a regular liquid box, up to 2 hours when large cutoffs and asymmetry indices have to be calculated. For reproducibility, the source code, full documentation, sample inputs and outputs, and all the crucial frames of the trajectories are available from the author upon request at his e-mail address.

Results

Liquid and crystalline *n*-hexane

Table 2 shows the comparison between calculated properties and available experimental data[15–17] (see Fig. S2† for the corresponding temperature/property plots). The density of the liquid is accurately simulated, while calculated vaporization and sublimation enthalpies are equal to, or slightly larger than the experiment. The distribution of torsion angles in the liquid (Fig. S3†) has the expected spread with temperature, and at 160 K shows a 7 : 1 *trans*/*gauche* ratio, in broad agreement with the value of $\exp(-\Delta E/RT)$, with a ΔE of about 3 kJ mol^{-1}.[5] Center-of mass and atom–atom radial distribution functions are also in line with expectation for an equilibrium *n*-alkane liquid or crystal (they will be discussed in subsequent paragraphs, in comparison with those for the crystal and for the frames resulting from crystallization runs). The agreement between calculation and experiment reached in these preliminary simulations is satisfactory and demonstrates that the force field is adequate for a sound representation of the condensed phases of *n*-hexane.

Table 2 Calculated and observed properties of *n*-hexane. Densities in g cm^{-3}, energies in kJ mol^{-1}

	Density		Heat of transition	
Temperature/K	calc	obs	calc	obs
Liquid			Vaporization	
160	0.76	—	35.2	—
200	0.74	—	35.0	
240	0.71	—	33.2	
290	0.66	0.660[a]	30.9	30–33[b]
Crystal			Sublimation	
158	—	0.900[c]	56.5	55.2[d]
90	—	0.888[e]		

[a] Ref. 15. [b] Ref. 16. [c] Ref. 2. [d] Ref. 17, at 0 K. [e] Ref. 18. See Table 3, later on, for detail of total energies.

Symmetrization runs, crystallization

The *n*-hexane crystal has half a molecule in the asymmetric unit so that the molecular and crystallographic centers of symmetry coincide.[2,18] Molecules in the crystal are parallel and elongated in an all-*trans* conformation ($\tau = 180°$) within experimental standard deviation. The final box from the simulation of liquid *n*-hexane at 160 K was used as the starting point of all symmetrization runs, always assigning a formal temperature of 160 K and a formal pressure of 1 atm. The system then evolves under the constraint of eqn (6), whereby the most straightforward way of decreasing the total asymmetry is to drive all molecules into all-*trans* conformations, as it turns out. Since in the latter conformation *n*-hexane is a centrosymmetric molecule, the two indices of eqn (3) and (4) coexist and cooperate to the symmetrization.

The asymmetry tolerance index T_s (the threshold increase in asymmetry for acceptance of a symmetrisation move) was first set at 10^{-6} and 10^{-5}, in 3 Mmove runs (1 Mmove = one million MC steps). The symmetrization algorithm is very efficient, and the decrease of the asymmetry index is very fast under these very stiff constraints. The resulting phases have all molecules elongated and parallel, in a sort of liquid-crystal-like or glassy arrangement (Fig. S4†). The trajectories (Fig. S5†) however show (i) large activation energy barriers of (respectively) 20 or 13 kJ mol^{-1} or a good part of the entire vaporization energy, (ii) an unrealistic increase in internal pressure to some 180 or 90 atm, and (iii) a 10 or 7% expansion of the whole system, due to the lack of sufficient relaxation time—although there is no time coordinate in a Monte Carlo-type simulation, as an order of magnitude, we estimate that 1 Mmove corresponds to half a picosecond. These runs were nonetheless useful because they indicate that when a stiffer symmetry constraint is set, the result is a quicker symmetrization but larger activation parameters; the system is forcedly driven across the hills of phase space rather than through more favourable valleys. In fact when T_s is set at 5×10^{-5} no symmetrization occurs and the system is simulated as an isotropic liquid. This value is therefore established as the upper practical limit for T_s.

Following the above preliminary indications, a continuous crystallization trajectory was planned in consecutive steps of 10 Mmoves each, assuming a fair balance between efficiency of the symmetrization (small tolerance) and relaxation time allowance (high tolerance index), and considering that when the system is closer to the final target a stiffer constraint is less unrealistic. The

successive T_s values were therefore 3×10^{-5}, 2×10^{-5}, 2×10^{-5}, 1×10^{-5}, 5×10^{-6}, 1×10^{-6} and 5×10^{-7}, in runs labelled S1 to S7. The final result is shown in Fig. 1: the structure is in molecular layers with layer periodicity parameters $a = 4.1$, $b = 4.5$ Å, $\gamma = 75°$, almost identical to the parameters of the real structure (4.13, 4.69, 75.2). The layers are stacked (Fig. 2a) with a translation parameter $c = 9.4$ Å, slightly longer than in the experimental structure (8.54, Fig. 2b) where the molecular orientation within layers is slightly different. Total energies are also very similar (see Table 3). The density of our calculated structure is 0.82, slightly smaller than the experiment (0.88). Further optimization in the attempt of reaching closer to the experimental crystal structure was, however, not pursued because (i) an accurate reproduction of the experimental crystal structure would have required at the very least anisotropic pressure control, not possible in our present model; and (ii) in *n*-alkanes Coulombic energy is entirely penetration energy (energy deriving from interaction between diffuse electron clouds between molecules), intrinsically missing from point-charge models. In fact, the atom–atom Coulombic energy of the *n*-hexane crystal is +0.8 kJ mol^{-1}, while the correct Coulombic energy, as calculated by PIXEL,[19] is −10.7 kJ mol^{-1}. The hopes of appreciating a small energy difference between very similar crystal structures of fatty-chain systems are rather slim when atom–atom models are used.

The crystallinity of the final assembly in Fig. 1 can be probed in several ways. Fig. 3 shows the center-of-mass radial distribution functions (rdfs) of the true crystal in comparison with those from the end result of the various symmetrization steps: the graph shows a coalescence of the calculated rdf to the experimental one as the run advances. The final frame has peaks almost overlapping those of the real crystal, but detail in the 4–6 Å zone reveals a (not unexpected) lack of resolution, with a broad peak with shoulders for the calculated structure in place of the three-peak feature of the real structure. The same effect in evident in the comparison of atom–atom rdfs, those for the calculated structure being a low-resolution image of the experimental ones (Fig. S6†). In the same way, the Debye scattering profiles (Fig. S7†) show one broad peak for the calculated structure at about 12°, straddling a double-peak feature at 10 and 14° for the real structure. (These profiles are anyhow of very poor resolution, due to the limited number of contributing scatterers and the absence of true infinite periodicity.) The general conclusion from these comparisons is that the molecular aggregate produced by the simulation is definitely crystalline, albeit with a rather high degree of structural "fuzziness", more evident in the registry between layers than in the organization within the layers.

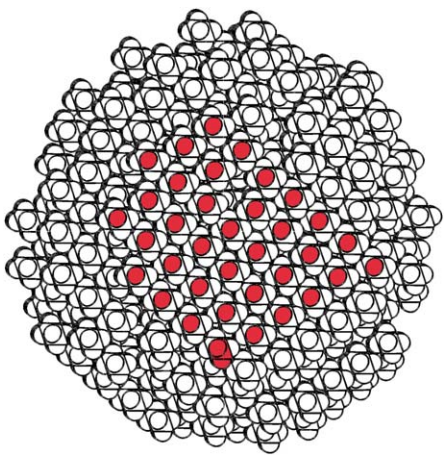

Fig. 1 Top view of a globular array from the final symmetric structure. The upward-pointing methyl hydrogen atoms of the top layer are shaded in red to show the layer periodicity.

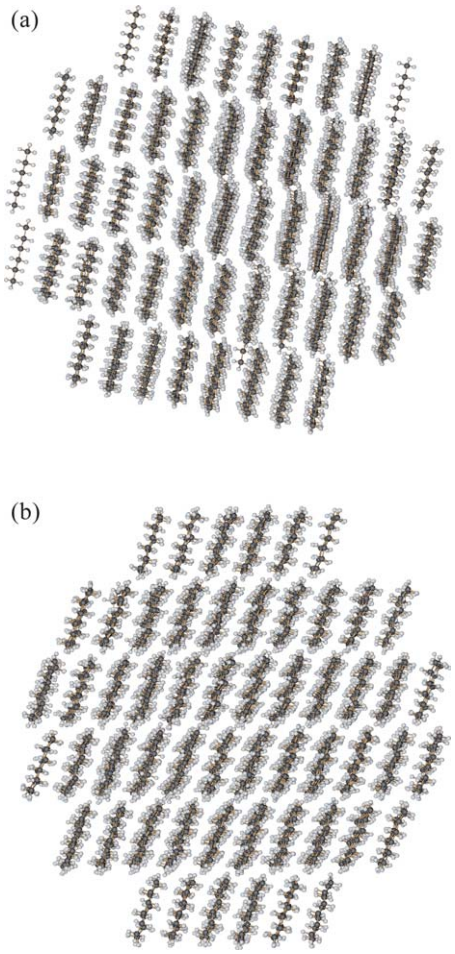

Fig. 2 (a) A side view of the globular array shown in Fig. 1. (b) The same from the simulation of the real crystal structure. The two frames show some difference in the orientation of molecules within the layers.

Table 3 Energy composition (kJ mol^{-1}) for the various phases: intramolecular, 6-exp (LJ), Coulombic, total energies. Notice the very small values of Coulombic energy

Phase	*E* (intra)	*E* (LJ)	*E* (coul)	*E* (tot)
160 K: liquid	9.2	−39.9	−0.1	−30.9
Crystal	2.0	−54.4	0.3	−52.2
Phase S7	−1.2	−50.5	−0.4	−52.1
Gas	3.1	—	—	3.1
Liq, 200 K	10.0	−38.5	−0.1	−28.6
Gas, 200 K	4.8	—	—	4.8
Liq, 240 K	11.5	−35.7	0	−24.4
Gas, 240 K	6.8	—	—	6.8
Liq, 290 K	13.2	−31.9	0	−18.8
Gas, 290 K	9.7	—	—	9.7

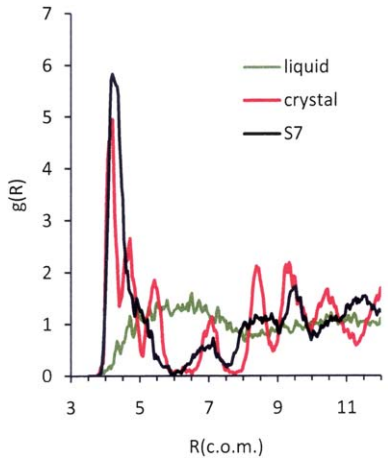

Fig. 3 The center-of-mass radial distribution function in the liquid, in the crystal, and after the last symmetrization step S7.

Crystallization trajectories

The analysis of the crystallization trajectory reveals more on the mechanism of crystallization. Fig. 4 shows that the transition from a population of *gauche* molecules to the all-*trans* conformations is accomplished in about 30 Mmoves, that is, very quickly. The poly-graphs of Fig. 5 show that whenever there is an acceleration of the symmetrization process due to the introduction of a stiffer T_s constraint, the system reacts by a rise in energy and pressure, with consequent expansion; all these effects become smaller as T_s becomes larger. By extrapolation one may surmise that a judicious choice of the sequence of symmetrization constraints would allow a crystallization path along which the energy barrier falls to such a small value as to merge into the thermal noise at the given temperature; already in our case the total energy barrier does not exceed 5 kJ mol^{-1}. The presence of an expansion also apparently contradicts the thermodynamic notion that $dP/dT > 0$ for the liquid–solid equilibrium of all substances (with the only known exception of water).

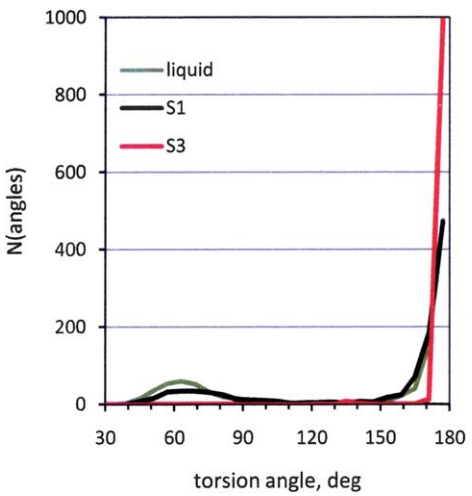

Fig. 4 The evolution of the distribution of torsion angles as symmetrization proceeds: the population of 60° torsions is practically zero after step S2.

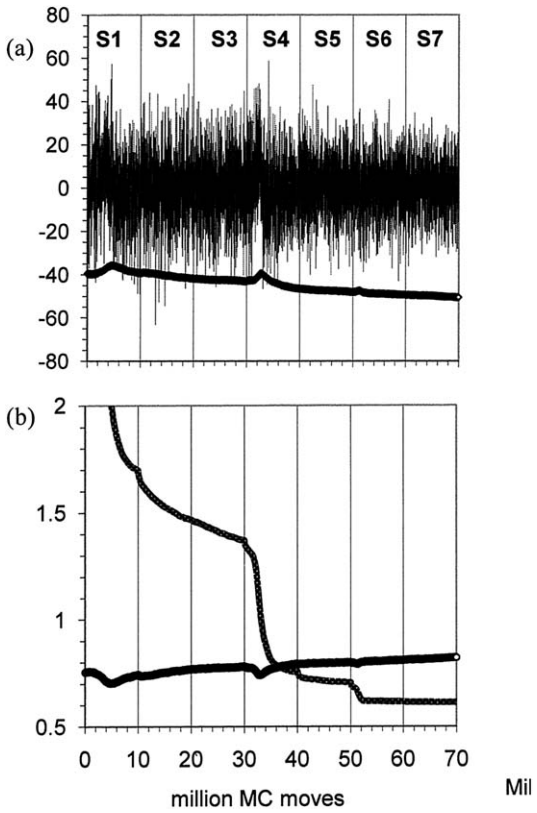

Fig. 5 (a) The evolution of pressure (atm; thin line) and of cohesive energy (kJ mol^{-1}; solid line). (b) The evolution of asymmetry index from 2.5 to about 0.7 (gray line), and of density (g cm^{-3}) from 0.66 to 0.82 (thicker black line). The two sharp drops in asymmetry index coincide with downward fluctuations in the density, and upward fluctuations in the pressure and energy.

Nevertheless, the result is chemically reasonable as a long and flexible molecule such as *n*-hexane may need extra space to uncoil from *gauche* to *trans*. We interpret the result of the simulation as an indication that during the complex kinetic events of crystallization, local density fluctuations might occur also in the direction of a density decrease, with a small price in energy. These fluctuations may be so small as not to affect the overall density of the real macroscopic sample.

Atomistic detail on the transformations that take place at the interface can be obtained using correlation functions (see ESI‡ for more details). Fig. 6 shows the translational correlation, or the mean squared displacement from a reference frame during a simulation. The advancement of the structuring and fixation that occurs during crystallization is displayed by the substantial decrease in displacements on going from stage S1 to S2 to S3, and the new increase at stage S4 where the symmetrization constraint is strengthened (check with Fig. 5). From stage S5 on, molecular translational displacement is extremely reduced, to 1 Å or less, somewhat larger than average values for a crystalline structure, and not far from the order of magnitude of liquid crystals. Rotational correlation is a number that goes from 1 (all molecular vectors equi-oriented) to zero (complete randomness in orientation). Rotational correlation is quenched much more quickly by the forced symmetrization (Fig. 7). In fact stage S1 still has much of the character of a liquid-state correlation

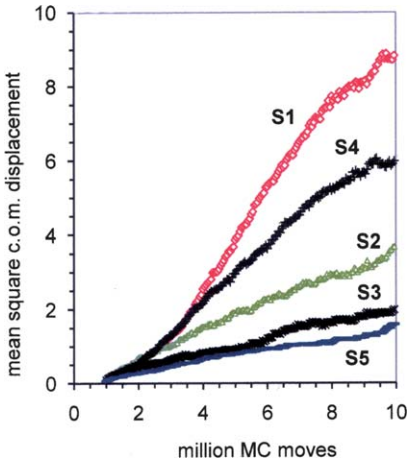

Fig. 6 Mean squared displacement of the centers of mass (Å^2) from a reference frame taken at 1 Mmove. Labels S1–S5 as in Fig. 5.

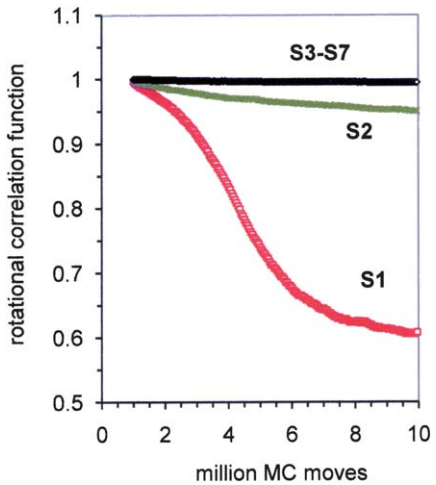

Fig. 7 Rotational correlation functions from a reference frame taken at 1 Mmove. Labels S1–S7 as in Fig. 5.

function, except for the incipient levelling at about 0.5, while from stage S3 on the alignment is practically complete, controlled by the strong symmetrization bias. The smoothness of all traces in Fig. 6 and 7 points to a continuous transition from isotropic liquid to crystal anisotropy without formation of grains or islands; this behaviour is also to some extent predetermined by the randomness of the computational moves, which are made to occur on an isotropic grid within the computational box.

Discussion and outlook

Can a computer crystallize a liquid? This paper shows that the answer to this question is yes, albeit in company of a number of possibly artificial side results. Adherence to Monte Carlo simulation standards is a matter of debate. When the procedure is used without symmetrization constraints, there is full adherence to statistical mechanics prescriptions except for the treatment of pressure control (it has, however, been checked, using a modified version of the present software,[14] that for pure liquids the results obtained using the standard isothermal–isobaric ensemble[10] are practically identical to those obtained here). When the symmetry constraint is enforced the algorithm leads the system in the desired direction very efficiently, but drifts apart from the regular NPT sampling procedure as the system drifts apart from equilibrium conditions. In future developments one could possibly devise a "force constant" for symmetrization with a corresponding partition function, in order to define a more rigorous statistical probability of acceptance over the symmetry index. The symmetry bias is also somewhat in conflict with the definition of temperature in the Monte Carlo environment, because only certain vibrations are allowed. This is the price that must be paid for tracing a crystallization trajectory in a comparatively small amount of computing time, in fact, accessible to nearly any computing facility. Using a strict bias, a crystal structure can be generated from the liquid in a time lapse almost adaptable to extensive crystal structure generation procedures such as are necessary for computer crystal structure prediction (CSP). This opens an entirely new pathway with respect to the usual structure generation for CSP.[20]

Are the trajectories reliable? One is never too cautious in drawing conclusions from molecular simulations, especially those that include a number of artificial constraints and therefore stray far from equilibrium conditions. Our present study shows how to map some channels through configuration space that connect isotropic molecular assemblies (liquids) with strongly anisotropic, very nearly or completely crystalline states, and puts an upper limit to the involved internal energy barriers. Such channels require sometimes an increase in internal pressure and a transient decrease in density. While the existence of other pathways involving even lower energy barriers cannot be ruled out (their existence is indeed very likely), once the barriers have dropped at or below the level of available thermal energy at a given temperature, the overcoming of the barriers becomes more and more likely and the adoption of the corresponding trajectories more and more probable. Our simulations suggest that as the difference in chemical potential (here represented by the symmetry bias) drives the advancement of the crystallization process, local fluctuations in internal energy and density are not unlikely. The smoothness of the plotted correlation functions suggests a uniform transition mode in which the molecules at random change their conformation and are directed towards the crystalline arrangement. Alternatively, some collective motion must be postulated, presumably at an even higher conceptual price.

What happens next? Prolongation of the simulation beyond the final point reached here was probed by short test runs. The cohesive energy of the system evolves to more stabilizing values extremely slowly, together with a very slow increase of density. If simulation conditions (force field, temperature and pressure control) were perfect, and the simulation was prolonged for an infinite time, the system most likely would reach as a final destination the exact experimental crystal structure of *n*-hexane. The working hypothesis that may be inferred by the overall deployment of the simulation is that a highly organized, liquid-crystal-like configuration is reached rather quickly, while the final "clicking" into the precise crystalline arrangement requires much more time. Gross molecular correlation is, perhaps not unexpectedly, easier to reach than the fine adjustments that are necessary for the adoption of a precise symmetry relationship.

How general are the conclusions reached? The results presented here are in a way preliminary, a term which we take in the positive signification of "suggestive of development", rather than in the negative sense of "incomplete". Test calculations show that the same general behaviour is observed in simulations with other materials, with different force fields and with other temperature or pressure protocols. Thus, the effects reported here cannot be a complete computational artifact pertaining to the chosen system or to the chosen boundary conditions. There is hardly any doubt that an energetically viable and chemically reasonable trajectory has been mapped through phase space. It is not clear if and how the derived predictions might be tested experimentally. Anyway the best value of the simulation is that it provides truly *a priori* computational suggestions that can in turn suggest the design of new experimental attempts, and eventually help in the development of new theories on the crystallization process.

The approach described in the present paper may be refined in the numerical formulation of the asymmetry indices, and in the optimization of the simulation conditions (among others, steps, tolerances, timing, choice of temperature ranges and possible annealing). Tests have shown that the algorithm works also in binary systems, where asymmetry is gauged among solutes only, thus opening the way to the study of aggregation from solution. Better potentials, and extension to screw axis and glide plane symmetry are being developed.[21] Ideally, however, a global order parameter describing the lattice point distribution and the "amount of crystallinity" in a given molecular ensemble should be devised. This goal, rather easy to reach with model systems like ensembles of monoatomic or globular entities, remains for the moment highly elusive for the real polyatomic and conformationally flexible molecules of everyday chemistry.

Acknowledgements

Structural drawings of Fig. 1 and 2 were prepared using program Schakal.[22]

References

1 M. A. Lovette, A. R. Browning, D. W. Griffin, J. P. Sizemore, R. C. Snyder and M. F. Doherty, *Ind. Eng. Chem. Res.*, 2008, **47**, 9812.
2 R. Boese, D. Blaeser and H.-C. Weiss, *Angew. Chem., Int. Ed.*, 1999, **38**, 988.
3 For a perspective of free energy methods for the simulation of chemical equilibria see D. Kofke and D. Frenkel, Perspective: Free Energies and Phase Equilibria, in *Handbook of Materials Modeling*, ed. S. Yip, Springer, Dordrecht, 2005.
4 (*a*) J. Anwar, P. K. Boateng, R. Tamaki and S. Odedra, *Angew. Chem., Int. Ed.*, 2009, **48**, 1596; (*b*) H. J. Huang, W. Lu and L. S. Bartell, *J. Phys. Chem.*, 1996, **100**, 14276.
5 G. D. Smith and R. L. Jaffe, *J. Phys. Chem.*, 1996, **100**, 18718.
6 V. Ferretti, P. Gilli and A. Gavezzotti, *Chem.–Eur. J.*, 2002, **8**, 1710.
7 E. S. Ferrari, R. C. Burton, R. J. Davey and A. Gavezzotti, *J. Comput. Chem.*, 2006, **27**, 1211.
8 A. Gavezzotti and G. Filippini, *J. Phys. Chem.*, 1994, **98**, 4831.
9 A. Gavezzotti, *CrystEngComm*, 2008, **10**, 389.
10 (*a*) M. P. Allen and D. J. Tildesley, *Computer Simulation of Liquids*, Oxford University Press, Oxford 1989, p. 41, 123ff; (*b*) W. L. Jorgensen, J. Chandrasekhar and J. D. Madura, *J. Chem. Phys.*, 1983, **79**, 926.
11 W. F. van Gunsteren and H. J. C. Berendsen, *Angew. Chem., Int. Ed. Engl.*, 1990, **29**, 992.
12 Ref. 10*a*, p. 204; see also ref. 7.
13 See *e.g.*: *Fundamentals of Crystallography*, ed. C. Giacovazzo, Oxford University Press, Oxford 2002, p. 268ff.
14 A. Gavezzotti, *New J. Chem.*, 2011, DOI: 10.1039/c0nj00982b.
15 R. A. Khairulin, S. V. Stankus and V. A. Gruzdev, *Int. J. Thermophys.*, 2007, **28**, 1245.
16 NIST Webbook: http://webbook.nist.gov/chemistry.
17 L. L. Shipman, A. W. Burgess and H. A. Scheraga, *J. Phys. Chem.*, 1976, **80**, 32.
18 N. Norman and H. Mathisen, *Acta Chem. Scand.*, 1961, **15**, 1755.
19 A. Gavezzotti, *Mol. Phys.*, 2008, **106**, 1473.
20 M. A. Neumann, F. J. J. Leusen and J. Kendrick, *Angew. Chem.*, 2008, **120**, 2461.
21 A. Gavezzotti, *The Coulomb–Londond–Pauli (CLP) Model of Intermolecular Interaction, A Computer Program Package Including Atom–Atom and PIXEL Energies and Monte Carlo Modules, User's Manual*, University of Milano, 2010, See also ref. 14. Available from the author upon request at his e-mail address.
22 E. Keller, *SCHAKAL92, A Program for the Graphic Representation of Molecular and Crystallographic Models*, University of Freiburg, 1993.